ADVANCED FUNCTIONAL MATERIALS
www.afm-journal.de

Surface Chemistry Routes to Modulate the Photoluminescence of Graphene Quantum Dots: From Fluorescence Mechanism to Up-Conversion Bioimaging Applications

*Shoujun Zhu, Junhu Zhang, Shijia Tang, Chunyan Qiao, Lei Wang, Haiyu Wang, Xue Liu, Bo Li, Yunfeng Li, Weili Yu, Xingfeng Wang, Hongchen Sun, and Bai Yang**

The bandgap in graphene-based materials can be tuned from 0 eV to that of benzene by changing size and/or surface chemistry, making it a rising carbon-based fluorescent material. Here, the surface chemistry of small size graphene (graphene quantum dots, GQDs) is tuned programmably through modification or reduction and green luminescent GQDs are changed to blue luminescent GQDs. Several tools are employed to characterize the composition and morphology of resultants. More importantly, using this system, the luminescence mechanism (the competition between both the defect state emission and intrinsic state emission) is explored in detail. Experiments demonstrate that the chemical structure changes during modification or reduction suppresses non-radiative recombination of localized electron-hole pairs and/or enhances the integrity of surface π electron network. Therefore the intrinsic state emission plays a leading role, as opposed to defect state emission in GQDs. The results of time-resolved measurements are consistent with the suggested PL mechanism. Up-conversion PL of GQDs is successfully applied in near-IR excitation for bioimaging.

1. Introduction

For several decades, carbon-based fluorescent materials, primarily including carbon dots,[1–12] nanodiamonds,[13] fluorescent carbon nanotubes,[14] and fullerene,[15] have been the focus of advanced scientific researches. In recent years, the rising fluorescent graphene (FG) are attracting increasingly intense attention among chemists and material scientists, depending on their exceptional advantages such as large optical absorptivity, chemical stability, fine biocompatibility as well as low toxicity.[16–18] These superiorities in FG distinguish themselves from traditional fluorescent materials, making them perfect candidates for numerous exciting applications: bioimaging,[19] medical diagnosis,[17] catalysis,[20] photovoltaic devices,[21] etc.

In spite of the strong points we have mentioned above, unfortunately, intrinsic graphene is a zero-band semiconductor, which is difficult to be directly exploited as a fluorescent material. To open up the bandgap and facilitate applications, researchers usually change the surface chemistry of intrinsic graphene or convert it to 0D graphene quantum dots (GQDs).[22] Based on the two major strategies, currently, research works have allowed FG to be produced by approaches ranging from simple oxidation to cutting carbon sources and organic synthesis starting from small molecules. Specifically, many groups have obtained fluorescent graphene oxide (GO) by modified Hummers methods, surface oxygen plasma treatment, one-pot electrochemistry method, separation of carbon sources, etc.[23–34] GQDs with blue or green photoluminescence have been prepared by cutting graphene or other carbon sources (e.g., nanotubes, carbon fibers, C_{60}).[35–44] Dai's group reported the preparation of fluorescent nano-GO by rate separation method.[45] Also, recently, Müllen's and Li's groups have reported series of researches centered on solution-based synthetic routes to obtain GQDs with better stability and more uniform chemistry structure.[46–51]

Although much progress has been made, many more problems need solving before we can feasibly employ FG in large-scale productions. A major challenge is to obtain luminescence tunable GQDs with much higher quantum yields. This requires not only exquisite synthesis strategies but also clarifying the mystery of PL mechanism in FG. Previous reports indicate that luminescence mechanism may derive

S. Zhu, Prof. J. Zhang, S. Tang, X. Liu, B. Li, Y. Li, Dr. W. Yu, X. Wang, Prof. B. Yang
State Key Laboratory of Supramolecular Structure and Materials
College of Chemistry
Jilin University
Changchun, 130012, P. R. China
E-mail: byangchem@jlu.edu.cn
C. Qiao, Prof. H. Sun
School of Stomatology
Jilin University
Changchun, 130041, P. R. China
L. Wang, Prof. H. Wang
State Key Laboratory on Integrated Optoelectronics
College of Electronic Science & Engineering
Jilin University
Changchun, 130012, P. R. China
Dr. W. Yu
College of Material Science and Engineering
Changchun University of Science and Technology
Changchun, 130022, P. R. China

DOI: 10.1002/adfm.201201499

from quantum size effect, zig-zag sites and defect effect (energy traps).[16,19,35] Typically, quantum size effect and zig-zag sites can be classified as intrinsic state emission while the defect effect is ranged as defect state emission. In addition, intrinsic state emission can also be induced by recombination of localized electron-hole pairs.[27] In general, PL of GQDs is attributed to combining effect of intrinsic emission and defect emission, whereas at present, competition between both sides still needs detailed analysis and experiments. Also importantly, exploiting FG to practical applications in devices (e.g., solar cells, transistors, etc), catalysis, detection and biomedical fields need further investigation and optimization. For example, most formerly reported applications in bioimaging used luminescence induced by one-photon UV or blue excitations which are harmful to living cells or biosystems. Long-term PL and near-IR excitation are critically needed in biolabeling researches.

In our previous work, using a two-step method combining solvothermal synthesis and column chromatography separation, GQDs with different oxidation degrees were separated and controllable fluorescence was obtained. The green PL was considered to be induced by defect state emission.[19,44] Inspired by this process, in this chapter, we used the major products of the two-step method (the third component) as initial ingredients to rule out the effect of surface chemistry. Either through modification or reduction, we specifically modulate the surface chemical groups and investigate the effect of surface chemistry on PL behaviors. For surface modification, alkylamines were connected to GQDs (m-GQDs) and resulting m-GQDs possessed blue luminescence. Upon reaction, previously existed -COOH and epoxy, that always induce non-radiative recombination of localized electron-hole pairs and hold back the intrinsic state emission,[28] were replaced by -CONHR and -CNHR. The newly appeared groups can suppress of non-radiative process and thus enhance intrinsic state emission. On the other hand, $NaBH_4$ was used for the reduction case and blue luminescent r-GQDs were obtained. During this process, carbonyl, epoxy and amide moieties were transformed into -OH accompanied by decreased surface defects. Appearance of -OH not only removed non-radiative recombination but also enhanced the integration of π conjugated system of GQDs as an electron donator. Consequently, intrinsic state emission also plays the leading role in r-GQDs instead of defect state emission. The results of time-resolved measurements are further consistent with the suggested PL mechanism. Apart from performing the surface chemistry reactions and investigating their suggestive PL mechanism, the up-conversion PL of GQDs was successfully applied in near-IR excitation for bioimaging using two or multiphoton luminescence.

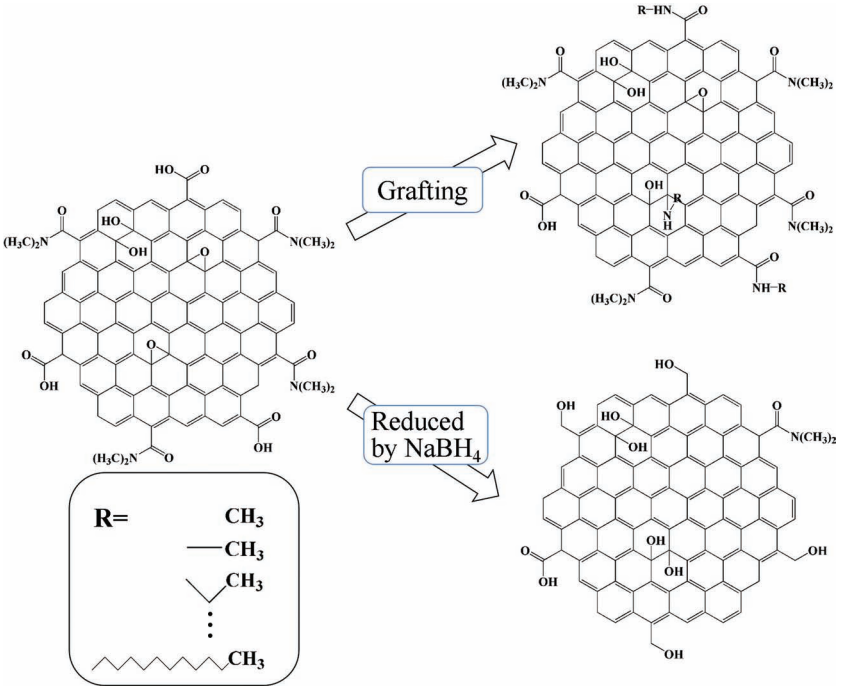

Figure 1. Scheme of preparation routes (suggested structures). m-GQDs are obtained by connecting with alkylamines, r-GQDs are obtained by reducing GQDs using $NaBH_4$.

2. Results and Discussion

2.1. Synthesis of GQDs with Controllable Surface Chemistry and Tunable PL Properties

As a major ingredient, green luminescent GQDs were obtained by a two-step solvothermal and separation method in our previous report.[19,44] The resulting GQDs have relatively high oxygen content with epoxy and -OH on molecular plane, $-CON(CH_3)_2$ and -COOH on edge. These active chemical groups endow them capability of being modified by organic molecules or polymers to regulate surface chemistry and thus changing the properties of GQDs programmably. Based on this principle, GQDs with controllable surface chemistry were obtained through chemical modification (m-GQDs) or reducing (r-GQDs), as shown in **Figure 1**. The m-GQDs were obtained by alkylamine coupling within a series of reactions (Figure S1, Supporting Information). Likewise, the r-GQDs were obtained by $NaBH_4$ reducing, during which carbonyl, epoxy and amide moieties were selectively reduced to hydroxyl groups while amide nearly disappeared.[12]

Several instrumentation tools were adopted to confirm successful modification or reduction. In FT-IR analysis of GQDs, m-GQDs (methylamine-GQDs was used as an example) and r-GQDs (**Figure 2**a), stretching vibrations of C-OH at 3430 cm^{-1}, C-H at 2923 cm^{-1} and 2850 cm^{-1} were observed in all three kinds of GQDs. However, asymmetric stretching vibration of C-NH-C at 1126 cm^{-1} and bending vibration of N-H at 1570 cm^{-1} were only observed in m-GQDs due to the attached methylamines. Justifiably, these analysis results confirmed the successful modification of GQDs. In addition, vibrational absorption band

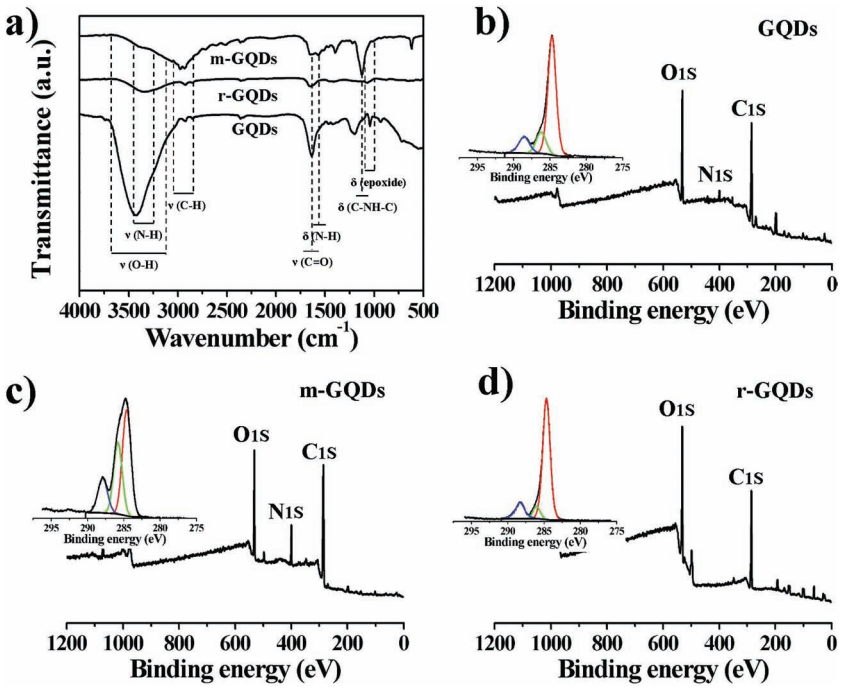

Figure 2. a) IR spectra of GQDs, m-GQDs and r-GQDs. b–d) XPS of GQDs, m-GQDs and r-GQDs.

of C=O at 1635 cm^{-1} shifted to 1652 cm^{-1} after reducing, accompanied by reduced intensity; while epoxide band at 1048 cm^{-1} completely disappeared in r-GQDs. These changes indicated the reduction of carbonyl and epoxide groups in r-GQDs. Moreover, surface changes in each case were also proved by XPS analysis (Figure 2b–d). After connecting with methylamines, a distinct increase in content of nitrogen was observed due to the coupling reactions. After reducing by $NaBH_4$, content of oxygen increased and that of nitrogen disappeared. Furthermore, the C1s analysis revealed the changes of percentage in three different carbons: graphitic carbon (C=C and C-C), oxygenated carbon and nitrous carbon (Table S1, Supporting Information). Compared to GQDs, percentage of graphitic carbon increases in r-GQDs, percentage of nitrous C disappeared in r-GQDs and increased in m-GQDs, substantiating successful reduction and modification process, respectively. The elemental analysis of GQDs, m-GQDs and r-GQDs also gave the contents C, O and N quantitatively (Table S2, Supporting Information), which is consistent with XPS results. From MALDI-TOF MS spectra of GQDs (Figure S2, Supporting Information), the molecular weights were in ca. 700–3500 with 24 interval (two carbons). However, since MALDI-TOF MS spectra have wide distributions, it is hard to determine the accurate molecular formula though the molecular weights and chemical groups were confirmed.

Morphology characterization demonstrates that GQDs possess 3.2 nm diameter and 1.02 nm height (**Figure 3**a,d), m-GQDs possess 3.6 nm diameter and 1.96 nm height (Figure 3b,e). The increase in morphology parameters attributes to the connection of methylamine and m-GQDs modified by alkylamines with increasing chain length possess increased diameters and heights (not shown here). In contrast, r-GQDs possess 3.1 nm diameter and 0.94 nm height (Figure 3c,f). Similar diameters and heights in GQDs and r-GQDs is owing to similar sizes of chemical groups before and after reduction. Furthermore, high-resolution transmission electron microscope (HTEM) shows that the three kinds of GQDs have crystallinity with lattices of 0.24–0.31 nm (insets of Figure 3a–c). These lattices may be sp^2 clusters in GQDs or carbon quantum dots obtaining in the solvothermal route.[19]

Optical properties of GQDs, m-GQDs and r-GQDs were measured to reveal effect of surface chemistry on PL behaviors (**Figure 4**). In UV-Vis spectra, the shoulder peak shifts from 320 nm in GQDs to about 330 nm in m-GQDs and r-GQDs, owing to surface

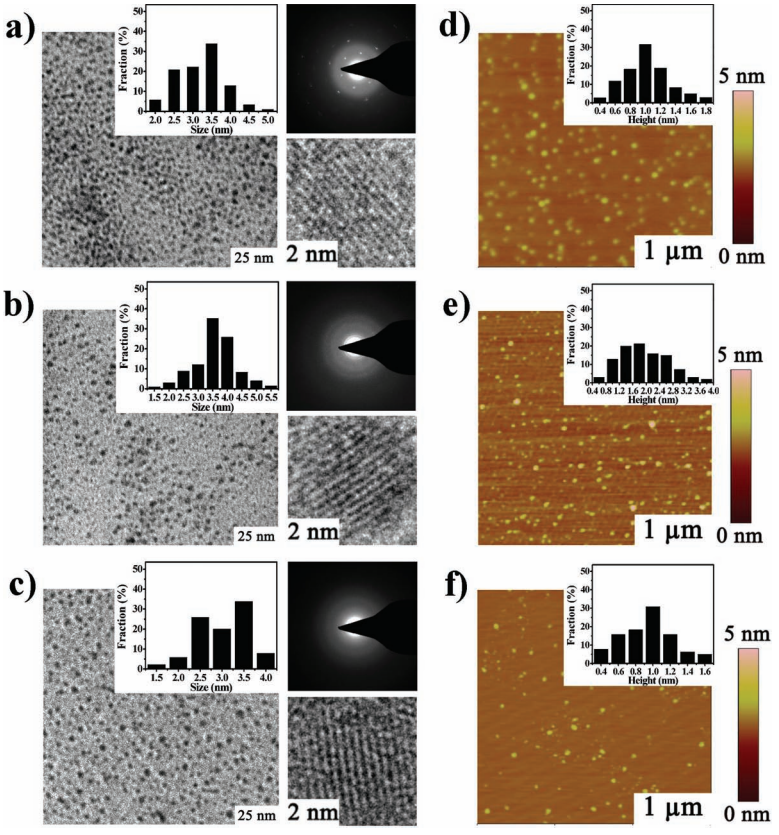

Figure 3. Morphology of GQDs. a–c) Transmission electron microscopy (TEM) images of GQDs, m-GQDs and r-GQDs, respectively. Inset images are size distributions, selected area electron diffraction and HTEM images. d–f) Atomic force microscopy (AFM) images of GQDs, m-GQDs, and r-GQDs respectively. Inset images are height distributions.

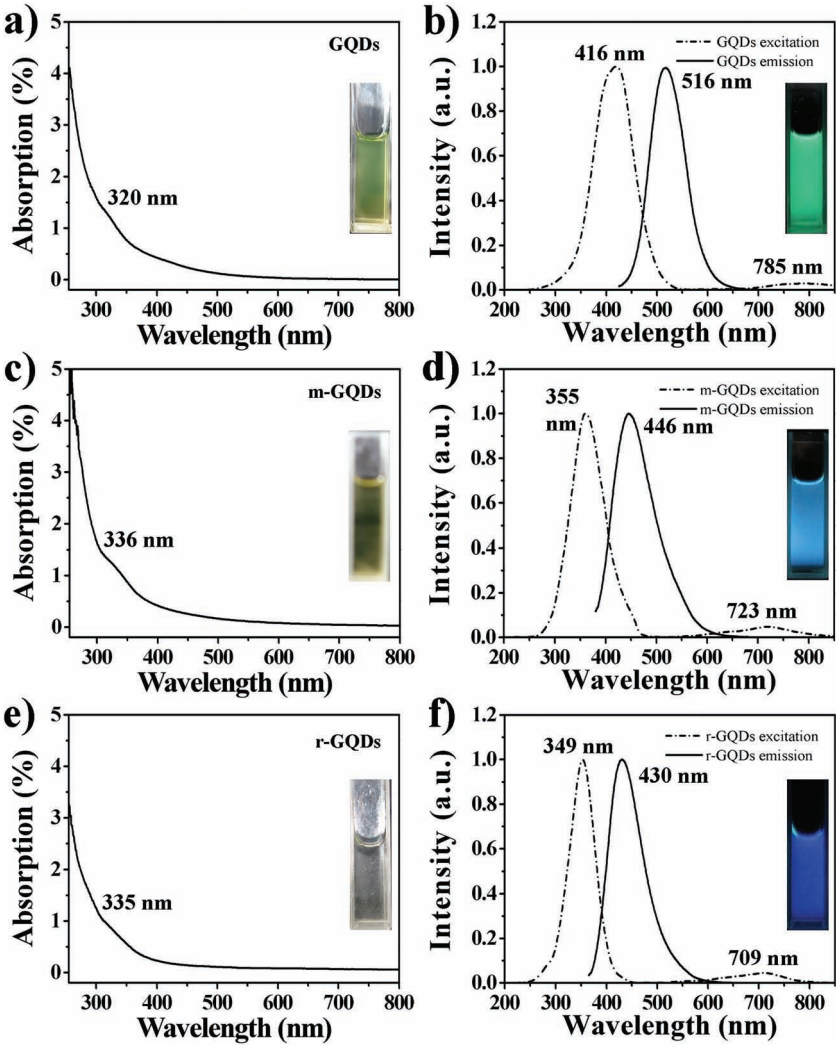

Figure 4. The optical properties of a,b) GQDs, c,d) m-GQDs, e,f) and r-GQDs aqueous solutions. a,c,e) UV-Vis absorption (ABS) spectra (inset: photographs taken under visible light). b,d,f) Optimal excitation and emission PL spectra (inset: photographs taken under 365 nm UV ligtht).

passivation of methylamine and electron enriching, respectively.[27] In fluorescence spectra, starting GQDs have optimal excitation and emission wavelengths at 416 nm and 516 nm, and show green color under handy UV lamp. However, these values blue shift to 355 nm and 446 nm for m-GQDs, 349 nm and 430 nm for r-GQDs. And both m-GQDs and r-GQDs show blue color under handy UV lamp. Also noteworthy, the optimal up-conversion excitation wavelength also blue shifts from 785 nm in GQDs to 723 nm in m-GQDs and 709 nm in r-GQDs (also see up-conversion PL in **Figure 5**).

Excitation-dependent PL behaviors are common in fluorescent carbon materials.[2–16] They afford multi-PL colors under different excitation wavelengths and this property is important for certain practical applications. The initial GQDs show a strong peak at 436 nm (blue emission) as well as a shoulder peak at 516 nm (green emission) when excited under 320 nm wavelength (Figure 5a). With redshift of the excitation wavelength, the peak at 436 nm decreases to disappear while the one at 516 nm increases remarkably. For m-GQDs and r-GQDs under 320 nm excitation, only blue emission left (Figure 5c,) and the emission wavelengths also redshift with increased excitation wavelengths. The up-conversion PL behaviors of GQDs, m-GQDs or r-GQDs are similar to the down-conversion excitation-dependent PL behaviors of their counterparts. In Figure 5b,d,f, the emission wavelengths redshift when changing excitation wavelengths from 600 to 900 nm. The up-conversion PL property is possibly attributed to the two or multiphoton active process.[39,44]

2.2. PL Mechanism Analysis of GQDs

Results enumerated above proved that the changes in PL behaviors from GQDs to m-GQDs or r-GQDs were induced by several PL mechanisms. To reveal this fluorescence mechanism, we tried to analyze the relationship between chemical structures and corresponding PL behaviors. Previous reports confirmed that defect state emission (surface energy traps) and intrinsic state emission (electron-hole recombination, quantum size effect/zig-zag sites) contribute to fluorescence synchronously.[11,16,19,27,35] In our experiments, initial green luminescent GQDs have two emission peaks, one is around 430–446 nm (blue emission) and the other one is at 516 nm (green emission). We speculated that the blue emission is attributed to electron-hole recombination or quantum size effect/zig-zag effect (intrinsic state emission), while the green emission is attributed to surface defects (defect state emission). To clarify this hypothesis, on one hand, we changed the surface chemistry of GQDs by methylamine coupling and blue fluorescent m-GQDs were obtained. The resultant groups (-CONHR and -CNHR) suppress of non-radiative process by passivating the initial epoxy and carboxylic groups, which always induce non-radiative recombination of localized electron-hole pairs and hold back pristine emission. That is, surface modification makes intrinsic state emission play the leading role in PL behaviors. On the other hand, GQDs were also transformed to blue luminescent r-GQDs after reducing. In this process, carbonyl, epoxy and amide moieties were changed into -OH groups, which suppress of non-radiative process and further enhance integrity of π conjugated system as an electron donator (also reduced the defects). Consequently, the intrinsic state emission plays the leading role in r-GQDs and only blue emission left. In general, both modification and reduction can tune GQDs surface chemistry groups and tailor the fluorescence color from green to blue, as shown in **Figure 6**. Also reasonably, r-GQDs have larger band gap than that of m-GQDs, owing to suppressing of non-radiative process as well as enriched electron

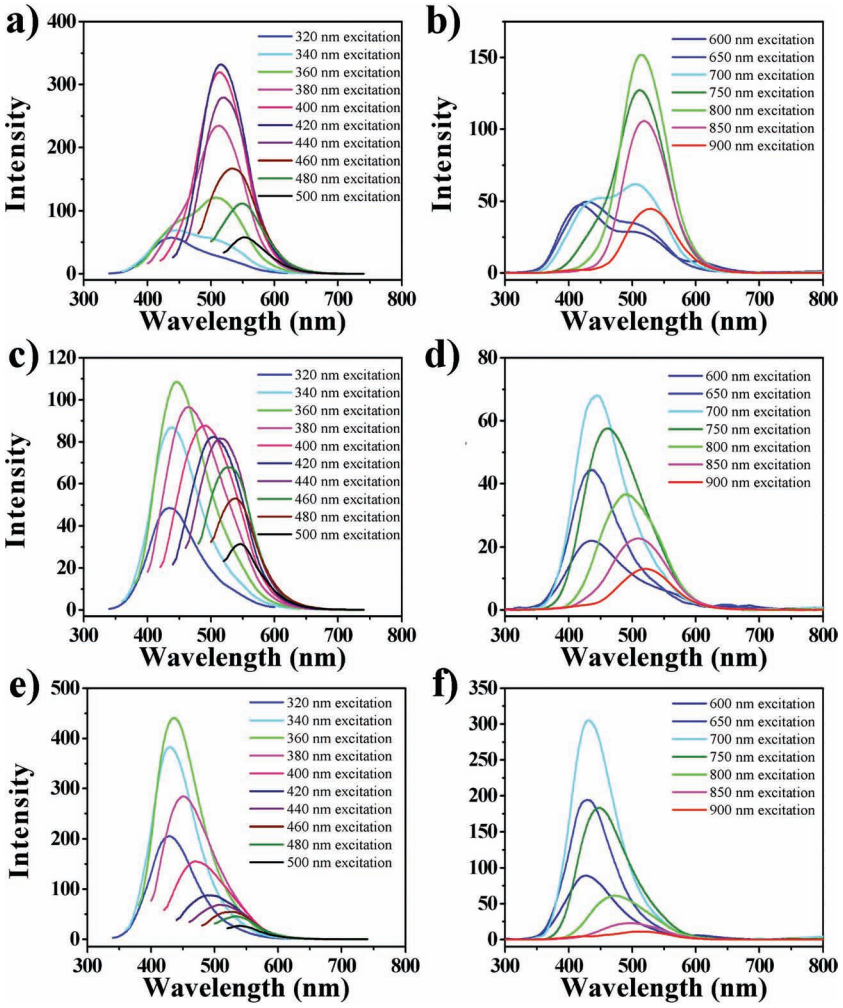

Figure 5. The excitation and up-conversion properties of a,b) GQDs, c,d) m-GQDs, and e,f) r-GQDs. a,c,e) The excitation-dependent PL behaviors. b,d,f) The up-conversion PL properties.

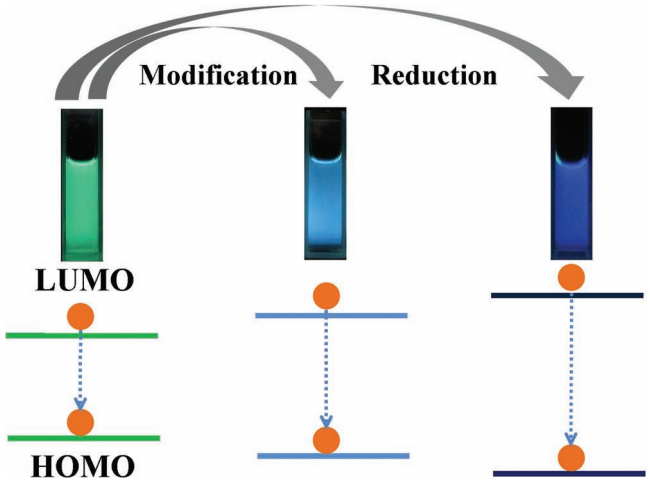

Figure 6. Scheme of bandgap changing of GQDs, m-GQDs and r-GQDs.

density caused by -OH groups. Enriched electron density was also bolstered by the distinct increase in quantum yield compared with r-GQDs and m-GQDs (Table S3, Supporting Information).

To further analyze the competition between intrinsic and defect state emission, ethylamine, propylamine, and other alkylamines were used to substitute methylamine (see supporting information). m-GQDs with similar surface chemistry but different modified chains were obtained. Interestingly, from Figure S3-S9 (Supporting Information), all m-GQDs with short alkyl chains have similar absorption, excitation-dependent PL (including down-conversion PL and up-conversion PL) and PL emissions, but exhibit enhanced hydrophobicity with increasing carbon numbers. This phenomenon suggests that nitrogen connecting rather than chain length of linear alkylamines (up to laurylamine in this paper) plays the major role in m-GQDs PL behaviors. That is, in this case, suppressing of non-radiative process induced by nitrogen is responsible for the transformation from green luminescence (GQDs) to blue luminescence (m-GQDs). However, when modifying PEG-NH_2, the PL behaviors of m-GQDs deviate from that when modifying small molecules (Figure S10, Supporting Information). This can be explained that long carbon chains with relatively few -NH_2 undermine the effect of nitrogen connection. Therefore, non-radiative recombination has not been effectively eliminated. That is, the defect state emission still plays the leading role in PEG-NH_2 modified GQDs. To further demonstrate the speculation above, again, we switched the modification agent to branched polyethlyenimine (PEI) with high nitrogen content (Figure S11, Supporting Information). In this case, effect of high nitrogen content competes over that of long carbon chains, thus tuning defect state emission to intrinsic state emission.

The pH-dependent and solvent-dependent PL behaviors also coincide with the proposed mechanisms. Due to ions or solvent attachment that induced emissive traps on surface of GQDs, only defect state emission was highly susceptible to environment changes while the intrinsic state emission was not. From **Figure 7**a, wavelength of PL peaks in r-GQDs nearly unchanged from pH 0 to 14, while that changed significantly in high pH range in GQDs. Additionally, since amide hydrolyzes in low pHs, different PL behaviors of m-GQDs were observed. In very low pH, some of the amide bonds broke, and the 516 nm emission appeared (see Figure S12a, Supporting Information), but the leading peak was still around 446 nm. In very high pH, amide groups of m-GQDs in alkali environment were stable and kept the blue emission (see Figure S12b, Supporting Information).[44] These phenomena proved that existence of amide bonds in m-GQDs was important to obtain the intrinsic

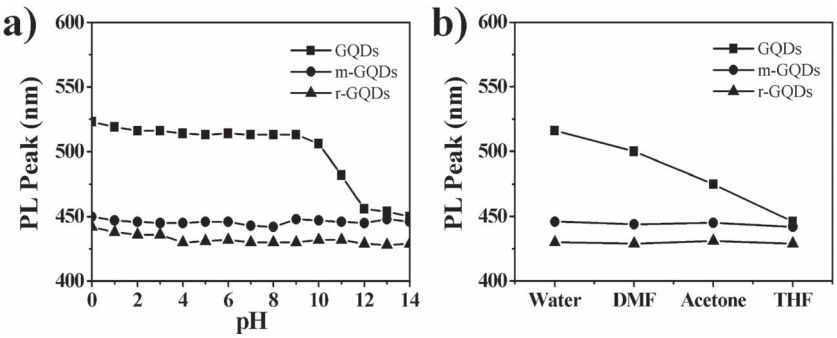

Figure 7. a) pH-dependent and b) solvent-dependent PL of GQDs, m-GQDs, and r-GQDs. PL peaks are collected at 380 nm excitation for GQDs and 360 nm excitation for m-GQDs and r-GQDs.

state emission. On the other hand, the PL of GQDs blueshift in solvent from water, dimethylformamide (DMF), acetone to tetrahydrofuran (THF), while m-GQDs and r-GQDs exhibited negligible solvent-dependent behaviors (Figure 7b).

It should note that the present surface chemistry routes to modulate the PL of GQDs are greatly different with previous work which reported the tunable fluorescence.[44] The separation method can only obtain the GQDs with different surface oxidations, and can not tune the surface groups programmable. However, in present work, through surface chemistry tuning, the PL of GQDs can be controlled devisably, and we can investigate the PL mechanism of GQDs in detail. Figure S13 (Supporting Information) shows the PL decay curves of GQDs, m-GQDs and r-GQDs. The average PL decay time of defect state emission (510–530 nm) decreases from 8.1 ns (for GQDs) to 3.5 ns for m-GQDs and 4.4 ns for r-GQDs, while the PL decay time of intrinsic state emission (420–450 nm) increases from 2.1 ns (for GQDs) to 2.7 ns for m-GQDs and 3.9 ns for r-GQDs. The changing PL decay time proved the transformation of defect state emission to intrinsic state emission from GQDs to m-GQDs and r-GQDs.

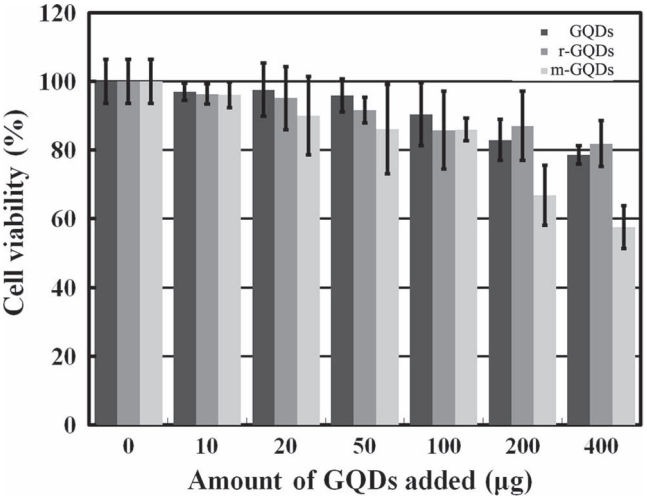

Figure 8. Effect of GQDs, m-GQDs, and r-GQDs on MC3T3 cells viability.

However, it is still necessary to innovate facile methods to GQDs with controllable surface chemistry, layers as well as sizes. Then rule out the PL mechanism among these effects. Further, the photophysics in GQDs should be also investigated by other ultrafast dynamics study from detailed microcosmic aspect.

2.3. Up-Conversion Bioimaging of GQDs

GQDs possess high stability, fine biocompatibility and low cytotoxicity which are promising in biological fields.[19] In vitro cytotoxicity of different GQDs contents was evaluated with MC3T3 cells by methylthiazolyldiphenyltetrazolium bromide (MTT) assay (**Figure 8**). Results suggest that GQDs and r-GQDs appeared very low toxicity to MC3T3 cells, with relative cell viability higher than 80% up to 400 μg adding. In marked contrast, m-GQDs show a distinct dose-dependent effect on cell viability. Over 40% cells were inhibitory when adding 400 μg m-GQDs. This difference may attribute to the connected methylamine, in which both nitrogen and alkyl chains affected the circumstance of cells.

Previous researches have demonstrated that GQDs are excellent biolabeling agents.[19,52,53] However, most formerly reported applications in bioimaging used luminescence induced by one-photon UV or blue excitations which are harmful to living cells or biosystems. The up-conversion PL of GQDs provided the advantage in harvesting near-IR light using multi-photon excitation.[20] This prompted us to explore their potential in cell labeling under near-IR multi-photon luminescence. From **Figure 9**, we can see bright green or blue area inside MC3T3 cells under near-IR excitation (808 nm), indicating successful translocation of GQDs through cell membrane. That is, without further bioconjugation, all three kinds of GQDs can penetrate living cells. Meanwhile, under continuous excitation over 20 min, no obvious reduction in PL brightness was observed, which indicates high photostability of GQDs. Surface hydrophilic groups, biological compatibility, strong and stable up-conversion PL make GQDs, m-GQDs and r-GQDs effective biological imaging platforms. Also, since graphene materials usually possess fewer layers (typically fewer than five layers) compared with other carbon-based fluorescent materials, it is more feasible to employ them in both scientific investigations and surface modifications for further biomedical applications.

3. Conclusions

We have developed a method to tune the photoluminescence of GQDs through surface chemistry and investigated their PL mechanisms. For m-GQDs, the connected alkylamines transferred the -COOH and epoxy of GQDs into -CONHR and -CNHR, both of which can reduce the non-radiative recombination and transfer GQDs from defect state emission into intrinsic state emission. While in reduction method to obtain r-GQDs, the carbonyl, epoxy and amido moieties were changed

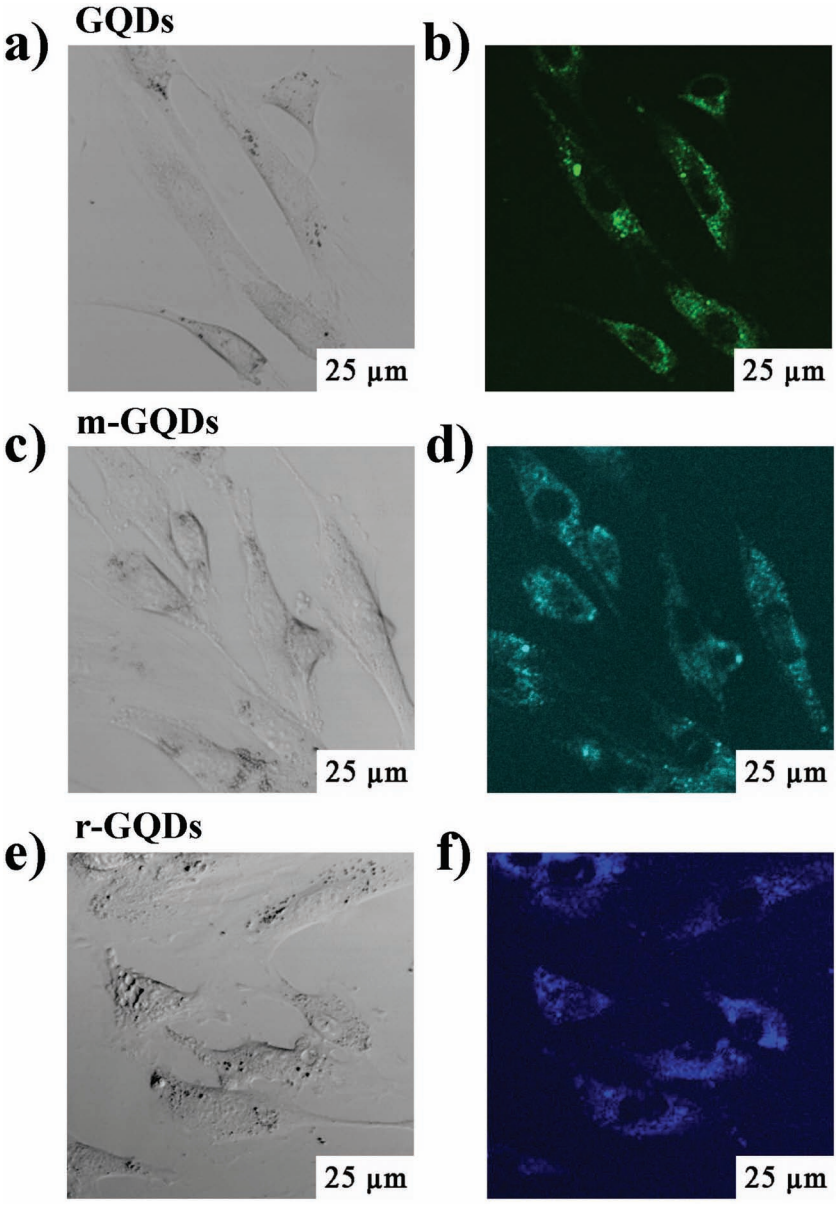

Figure 9. The up-conversion cellular imaging of GQDs: the washed cells imaged under bright field (a,c,e) and 808 nm excitation (b,d,f). The detection wavelength was in the 490–550 nm range for GQDs, 450–500 nm for m-GQDs, and 420–460 nm for r-GQDs.

into -OH groups, which suppress of non-radiative process and further enhance integrity of π conjugated system (also reduce the defects). As a result, intrinsic state emission plays the leading role instead of defect state emission. The results of time-resolved measurements are further consistent with the suggested PL mechanism. In sum, researches in this article provide a novel direction to synthesize GQDs with multi-color fluorescence through tuning surface chemistry.[54–57] Moreover, we give a deep insight into the relationship between structures and corresponding fluorescence and suggest a PL mechanism of GQDs. Due to the simple structure of GQDs, understanding their PL mechanism will provide inspiration for revealing PL mechanisms in other carbon-based fluorescent materials. Furthermore, successful up-conversion bio-imaging will prompted GQDs as a strong tool in many kinds of biomedical applications while avoiding harmful UV or blue excitations.

4. Experimental Section

Materials: Graphite power (<150 μm) and polyethylenimine (branched) were purchased from Aldrich. Alkylamines (methylamine, ethylamine, n-propylamine, n-butylamine, n-hexylamine, n-laurylamine, isopropylyamine, 1, 4-diaminobutane) were purchased from Aladdin or Sinopharm Chemical Reagent. NHS and EDC-HCl were purchase from Shanghai Medpep. $NaBH_4$ and PEG_{1000}-NH_2 were purchased from Sinopharm Chemical Reagent. Other chemicals were purchased from Beijing Chemical Works.

Preparation of GQDs: GQDs were prepared by reported methods.[19] Briefly, GO was dispersed in DMF with the concentrations of 50–270 mg/10 mL. The GO/DMF solutions were under ultrasonication for 30 minutes (120 W, 100 kHz), and then transferred to a poly (tetrafluoroethylene) (Teflon)-lined autoclave (30 mL) and heated at 200 °C for 8 h. After the above reaction, the reactors were cooled to room temperature by water or naturally. The product contained brown transparent suspension and black precipitates, and the black precipitates were wasted. The solid samples can be obtained by evaporating the solvents. Then, the GQDs were purified by column chromatography on silica utilizing gradient elution (mobile phase: A was Methylene Chloride-MeOH (2:1, V/V), B was H_2O). Under the A phase elution, two different batches were obtained in a sequence. Subsequently, under the B phase elution, another batch was obtained, which is the primary production with a yield of ca. 50–70% and was used in this paper.

Preparation of m-GQDs: GQDs aqueous (0.1–1 mg/mL) were added 500 μL EDC-HCl (10 mM) and NHS (5 mM) mixture, stirring at room temperature for 0.5 h. After that, 50 μL methylamine was added to the reaction system, stirring at room temperature for 4 h. Then, the reaction system was stirring at 40–100 °C for another 2 h to improve the reaction between methylamine and epoxy. The product was named as m-GQDs (see Figure S1, Supporting Information). The dominant functionality is -CONHR due to the initial proportion of -COOH and epoxy.[58] The other alkylamines, PEG-amine and PEI connected GQDs were obtained by the similar methods.

Preparation of r-GQDs: GQDs aqueous (0.1–1 mg/mL) were added 50 mg $NaBH_4$, the reaction was under stirring at room temperature for 4 h. After the reaction, the product was subjected to dialysis to completely remove ions (4 days, changed DI-water every 8 h). The result product was named as r-GQDs (see Figure 1).

Cellular Toxicity Test: Mouse osteoblastic cell line (MC3T3-E1) cells (10^4 cells/150 μL) were cultured first for 24 h in an incubator (37 °C, 5% CO_2), and for another 24 h after the culture medium was replaced with 100 μL of Dulbecco's modified Eagle's medium (DMEM) containing the GQDs, m-GQDs and r-GQDs at different doses (0, 10, 20, 50, 100, 200, 400 μg/mL). Then, 20 μL of 5 mg/mL MTT solution was added to every cell well. The cells were further incubated for 4 h, followed by removing the culture medium with MTT, and then 150 μL of DMSO was added.

The resulting mixture was shaken for ca. 5 min at room temperature. The optical density (OD) of the mixture was measured at 490 nm. The cell viability was estimated according to the following equation

$$\text{Cell } Viability\,(\%) = \left(\frac{OD_{\text{Treated}}}{OD_{\text{Control}}}\right) \times 100\%$$

where OD_{Control} was obtained in the absence of GQDs, and OD_{Treated} obtained in the presence of GQDs.

Cellular Imaging: The cells were cultured in DMEM supplemented with 10% fetal bovine serum and 1% penicillin/streptomycin. Suspensions (2.5 mg/mL) of GQDs from the stock solution were prepared with Dulbecco's phosphate buffer saline (DPBS). After sonication for 10 min to ensure complete dispersion, an aliquot (typically 0.1 mL) of the suspension was added to the well of a chamber slide, then incubated at 37 °C in a 5% CO_2 incubator for 20 h. Prior to fixation of the cells on the slide for inspection with a confocal fluorescence microscope, the excess GQDs were removed by washing 3 times with warm DPBS.

Characterization: High-resolution transmission electron microscope (HTEM) was recorded on FEI Tecnai F20. TEM was conducted using a Hitachi H-800 electron microscope at an acceleration voltage of 200 kV with a CCD cinema. AFM images were recorded in the tapping mode with a Nanoscope IIIa scanning probe microscope from Digital Instruments under ambient conditions. Fluorescence spectroscopy was performed with a Shimadzu RF-5301 PC spectrophotometer. UV-vis absorption spectra were obtained using a Shimadzu 3100 UV-vis spectrophotometer. IR spectra were taken on a Nicolet AVATAR 360 FT-IR spectrophotometer. The confocal microscopy images were taken at Olympus Fluoview FV1000. X-ray Photoelectron Spectroscopy (XPS) was investigated by using ESCALAB 250 spectrometer with a mono X-Ray source Al Kα excitation (1486.6 eV). Binding energy calibration was based on C_{1s} at 284.6 eV. Elemental analysis was performed on Elementar Vario MICRO CUBE, each data was parallel at least twice and the average values were obtained by measuring three kinds of sample batches. Matrix-assisted laser desorption/ionization reflect time-of-flight (MALDI-TOF) technique was recorded on Bruker autoflex speed TOF with tetracyanoquinodimethane (TCNQ) as the matrix.

Supporting Information

Supporting Information is available from the Wiley Online Library or from the author.

Acknowledgements

This work was supported by the National Science Foundation of China (Grand No. 91123031, 20921003, 50973039, 21074048). The authors thank Prof. Li Niu (Changchun Institute of Applied Chemistry, CAS, Changchun) for the GO preparation and helpful discussions. W.Y. acknowledges the Open Project of State Key Laboratory of Supramolecular Structure and Materials (SKLSSM 201223).

Received: June 4, 2012
Published online: July 20, 2012

[1] S. N. Baker, G. A. Baker, *Angew. Chem. Int. Ed.* **2010**, *49*, 6726.
[2] Y. Fang, S. Guo, D. Li, C. Zhu, W. Ren, S. Dong, E. Wang, *ACS Nano* **2012**, *6*, 400.
[3] X. Wang, L. Cao, S. T. Yang, F. Lu, M. J. Meziani, L. Tian, K. W. Sun, M. A. Bloodgood, Y. P. Sun, *Angew. Chem. Int. Ed.* **2010**, *49*, 5310.
[4] R. Liu, D. Wu, S. Liu, K. Koynov, W. Knoll, Q. Li, *Angew. Chem. Int. Ed.* **2009**, *48*, 4598.
[5] A. B. Bourlinos, A. Stassinopoulos, D. Anglos, R. Zboril, M. Karakassides, E. P. Giannelis, *Small* **2008**, *4*, 455.
[6] H. Liu, T. Ye, C. Mao, *Angew. Chem. Int. Ed.* **2007**, *446*, 6473.
[7] Q. L. Zhao, Z. L. Zhang, B. H. Huang, J. Peng, M. Zhang, D. W. Pang, *Chem. Commun.* **2008**, 5116.
[8] H. Zhu, X. Wang, Y. Li, Z. Wang, F. Yang, X.Yang, *Chem. Commun.* **2009**, 5118.
[9] D. Pan, J. Zhang, Z. Li, C. Wu, X. Yan, M. Wu, *Chem. Commun.* **2010**, *46*, 3681.
[10] H. Li, X. He, Z. Kang, H. Huang, Y. Liu, J. Liu, J. Liu, S. Lian, C. H. A. Tsang, X. Yang, S. T. Lee, *Angew. Chem. Int. Ed.* **2010**, *122*, 4532.
[11] L. Bao, Z. L. Zhang, Z. Q. Tian, L. Zhang, C Liu, Y. Lin, B. Qi, D. W. Pang, *Adv. Mater.* **2011**, *23*, 5801.
[12] H. Zheng, Q. Wang, Y. Long, H. Zhang, X. Huang, R. Zhu, *Chem. Commun.* **2011**, *47*, 10650.
[13] A. Krueger, *Adv. Mater.* **2008**, *20*, 2445.
[14] K. Welsher, Z. Liu, S. P. Sherlock, J. T. Robinson, Z. Chen, D. Daranciang, H. Dai, *Nat. Nanotechnol.* **2009**, *4*, 773.
[15] J. Jeong, M. Cho, Y. T. Lim, N. W. Song, B. H. Chung, *Angew. Chem. Int. Ed.* **2009**, *48*, 5296.
[16] K. P. Loh, Q. Bao, G. Eda, M. Chhowalla, *Nat. Chem.* **2010**, *2*, 1015.
[17] H. Shen, L. Zhang, M. Liu, Z. Zhang, *Theranostics* **2012**, *2*, e0013.
[18] J. Wang, X. Xin, Z. Lin, *Nanoscale* **2011**, *3*, 3040.
[19] S. Zhu, J. Zhang, C. Qiao, S. Tang, Y. Li, W. Yuan, B. Li, L. Tian, F. Liu, R. Hu, H. Gao, H. Wei, H. Zhang, H. Sun, B. Yang, *Chem. Commun.* **2011**, *47*, 6858.
[20] S. Zhao, M. Shao, S. T. Lee, *ACS Nano* **2012**, *6*, 1059.
[21] V. Gupta, N. Chaudhary, R. Srivastava, G. D. Sharma, R. Bhardwaj, S. Chand, *J. Am. Chem. Soc.* **2011**, *133*, 9960.
[22] S. Neubeck, L. A. Ponomarenko, F. Freitag, A. J. M. Giesbers, U. Zeitler, S. V. Morozov, P. Blake, A. K. Geim, K. S. Novoselov, *Small* **2010**, *6*, 1469.
[23] T. Gokus, R. R. Nair, A. Bonetti, M. Böhmler, A. Lombardo, K. S. Novoselov, A. K. Geim, A. C. Ferrari, A. Hartschuh, *ACS Nano* **2009**, *3*, 3963.
[24] T. V. Cuong, V. H. Pham, Q. T. Tran, S. H. Hahn, J. S. Chung, E. W. Shin, E. J. Kim, *Mater. Lett.* **2010**, *64*, 399.
[25] J. Chen, X. Yan, *J. Mater. Chem.* **2010**, *20*, 4328.
[26] Z. Luo, P. M. Vora, E. J. Mele, A. T. C. Johnson, J. M. Kikkawa, *Appl. Phys. Lett.* **2009**, *94*, 111909.
[27] G. Eda, Y. Y. Lin, C. Mattevi, H. Yamaguchi, H. A. Chen, I. S. Chen, C. W. Chen, M. Chhowalla, *Adv. Mater.* **2010**, *22*, 505.
[28] Q. Mei, K. Zhang, G. Guan, B. Liu, S. Wang, Z. Zhang, *Chem. Commun.* **2010**, *46*, 7319.
[29] Z. X. Gan, S. J. Xiong, X. L. Wu, C. Y. He, J. C. Shen, P. K. Chu, *Nano Lett.* **2011**, *11*, 3951.
[30] Z. Qian, J. Zhou, J. Chen, C. Wang, C. Chen, H. Feng, *J. Mater. Chem.* **2011**, *21*, 17635.
[31] J. Chen, X. Yan, *Chem. Commun.* **2011**, *47*, 3135.
[32] K. S. Subrahmanyam, P. Kumar, A. Nag, C. N. R. Rao, *Solid State Commun.* **2010**, *150*, 1774.
[33] G. Xin, H. Wang, N. Kim, W. Hwang, S. M. Cho, H. Chae, *Nanoscale* **2012**, *4*, 405.
[34] J. Lu, J. Yang, J. Wang, A. Lim, S. Wang, K. P. Loh, *ACS Nano* **2009**, *3*, 2367.
[35] D. Pan, J. Zhang, Z. Li, M. Wu, *Adv. Mater.* **2010**, *22*, 734.
[36] Y. Li, Y. Hu, Y. Zhao, G. Shi, L. Deng, Y. Hou, L. Qu, *Adv. Mater.* **2011**, *23*, 776.
[37] Y. Li, Y. Hu, Y. Zhao, G. Shi, L. Deng, Y. Hou, L. Qu, *J. Am. Chem. Soc.* **2012**, *134*, 15.
[38] H. Cheng, Y. Zhao, Y. Fan, X. Xie, L. Qu, G. Shi, *ACS Nano* **2012**, *6*, 2237.
[39] J. Shen, Y. Zhu, C. Chen, X. Yang, C. Li, *Chem. Commun.* **2011**, *47*, 2580.

[40] J. Shen, Y. Zhu, X. Yang, J. Zong, J. Zhang, C. Li, *New J. Chem.* **2012**, *36*, 97.
[41] J. Zhao, G. Chen, L. Zhu, G. Li, *Electrochem. Commun.* **2011**, *13*, 31.
[42] J. Peng, W. Gao, B. K. Gupta, Z. Liu, R. R. Aburto, L. Ge, L. Song, L. B. Alemany, X. Zhan, G. Gao, S. A. Vithayathil, B. A. Kaipparettu, A. A. Marti, T. Hayashi, J. J. Zhu, P. M. Ajayan, *Nano Lett.* **2012**, *12*, 844.
[43] J. Lu, P. S. E. Yeo, C. K. Gan, P. Wu, K. P. Loh, *Nat. Nanotechnol.* **2011**, *6*, 247.
[44] S. Zhu, J. Zhang, X. Liu, B. Li, X. Wang, S. Tang, Q. Meng, Y. Li, C. Shi, R. Hu, B. Yang, *RSC Adv.* **2012**, *2*, 2717.
[45] X. Sun, Z. Liu, K. Welsher, J. T. Robinson, A. Goodwin, S. Zaric, H. Dai, *Nano Res.* **2008**, *1*, 203.
[46] R. Liu, D. Wu, X. Feng, K. Müllen, *J. Am. Chem. Soc.* **2011**, *133*, 15221.
[47] J. Wu, W. Pisula, K. Müllen, *Chem. Rev.* **2007**, *107*, 718.
[48] X. Liang, W. Pisula, K. Müllen, *Pure Appl. Chem.* **2009**, *81*, 2203.
[49] L. Li, X. Yan, *J. Phys. Chem. Lett.* **2010**, *1*, 2572.
[50] X. Yan, X. Cui, L. Li, *J. Am. Chem. Soc.* **2010**, *132*, 5944.
[51] X. Yan, X. Cui, B. Li, L. Li, *Nano Lett.* **2010**, *10*, 1869.
[52] D. Pan, L. Guo, J. Zhang, C. Xi, Q. Xue, H. Huang, J. Li, Z. Zhang, W. Yu, Z. Chen, Z. Li, M. Wu, *J. Mater. Chem.* **2012**, *22*, 3314.
[53] M. Zhang, L. Bai, W. Shang, W. Xie, H. Ma, Y. Fu, D. Fang, H. Sun, L. Fan, M. Han, C. Liu, S. Yang, *J. Mater. Chem.* **2012**, *22*, 7461.
[54] A. B. Bourlinosa, V. Georgakilasa, R. Zborilb, A. Bakandritsosc, A. Stassinopoulosd, D. Anglosd, E. P. Giannelis, *Carbon* **2009**, *47*, 519.
[55] N. G. Shang, P. Papakonstantinou, S. Sharma, G. Lubarsky, M. Li, D. W. Mcneill, A. J. Quinn, W. Zhou, R. Blackley, *Chem. Commun.* **2012**, *48*, 1877.
[56] J. Shen, Y. Zhu, X. Yang, C. Li, *Chem. Commun.* **2012**, *48*, 3686.
[57] S. Zhu, S. Tang, J. Zhang, B. Yang, *Chem. Commun.* **2012**, *48*, 4527.
[58] The initial GQDs have both —COOH and epoxy groups, and the GQDs were obtained by the split of graphene oxide at defect positions, the quantity of —COOH at edge are more than epoxy in plane in GQDs. The dominant fuctionality is —CONHR due to the initial proportion of —COOH and epoxy.